Available online at www.sciencedirect.com
ScienceDirect
International Journal of Heat and Mass Transfer 51 (2008) 2377–2388
International Journal of HEAT and MASS TRANSFER
www.elsevier.com/locate/ijhmt

Treatment of turbulent heat fluxes with the elliptic-blending second-moment closure for turbulent natural convection flows

Seok-Ki Choi *, Seong-O Kim

Korea Atomic Energy Research Institute, Fluid System Engineering Division, 150 Deokjin-dong, Yuseong-gu, Daejeon 305-353, Republic of Korea

Received 6 April 2007; received in revised form 10 August 2007
Available online 24 October 2007

Abstract

In this paper a comparative study on the treatment of the turbulent heat fluxes with the elliptic-blending second-moment closure for natural convection flows is presented. Three different cases for treating the turbulent heat fluxes are considered. Those are the generalized gradient diffusion hypothesis (GGDH), the algebraic flux model (AFM) and the differential flux model (DFM). These models are implemented in a computer code especially designed for an evaluation of turbulent models. Calculations are performed for turbulent natural convection flows in an 1:5 rectangular cavity ($Ra = 4.3 \times 10^{10}$) and in a square cavity with conducting top and bottom walls ($Ra = 1.58 \times 10^{9}$). The calculated results are compared with the available experimental data. The results show that the GGDH, AFM and DFM models produce sufficiently accurate solutions for the turbulent natural convection in an 1:5 rectangular cavity where the strength of the thermal stratification is weak in a central region of the cavity. However, the GGDH model produces very erroneous solutions for the turbulent natural convection in a square cavity with conducting walls where the Rayleigh number is relatively small and the thermally stratified region is dominant. The AFM and DFM produce very accurate solutions for both cases without invoking any numerical problems.

Keywords: Turbulent natural convection; Elliptic-blending second-moment closure; General gradient diffusion hypothesis; Algebraic flux model; Differential flux model

1. Introduction

Accurate prediction of a natural convection is very important for investigating a fluid flow and heat transfer in various nuclear engineering applications such as the passive heat removal system of a liquid metal nuclear reactor. Until now the experimental data for the heat transfer coefficient of a natural convection in the passive heat removal system of a liquid metal nuclear reactor is very limited. Since the heat transfer coefficient depends on the geometry and the hydraulic and thermal conditions, it is more useful to evaluate the available turbulence models through an application to benchmark problems and to calculate the practical problems using the best turbulence model.

For natural convection flows, there exist little experimental data to test turbulence models, mainly due to experimental difficulties. It is still difficult to measure the turbulent heat fluxes and the low velocities accurately and to achieve the ideal adiabatic condition. The experimental data by Tsuji and Nagano [1] for a heated vertical flat plate, by King [2] and Cheesewright et al. [3] for a rectangular cavity, by Betts and Bokhari [4] for a vertical tall cavity, by Tian and Karayiannis [5] and Ampofo and Karayiannis [6] for a square cavity are examples of experimental data which have been used by many authors to test turbulence models and to validate their computer codes. The Large eddy Simulation (LES) by Peng and Davidson [7] for a natural convection in a square cavity for the experiment by Tian and Karayiannis [8] and by Kenjeres and

* Corresponding author. Tel.: +82 42 868 2993; fax: +82 42 861 7697.
E-mail address: skchoi@kaeri.re.kr (S.-K. Choi).

0017-9310/$ - see front matter © 2007 Elsevier Ltd. All rights reserved.
doi:10.1016/j.ijheatmasstransfer.2007.08.012

Hanjalic [9] for Rayleigh–Benard flow and the Direct Numerical Simulation (DNS) by Boudjemadi et al. [10], by Versteegh and Nieuwstadt [11] and by Worner and Grotzbach [12] are examples of the LES and DNS studies reported in the literatures. Most works in the literature employ the RANS (Reynolds Averaged Navier-Stokes) equation approach. In the RANS equation approach, the choice of a turbulence model is crucial, as it directly affects the accuracy of the solutions. However, the turbulence modeling of a natural convection is still difficult and the rationale for the difficulties is well explained in Hanjalic [13] and Dol et al. [14].

The earlier computations of natural convection were done by the standard k–ε model with wall function method. The examples of these calculations are due to Kuyper et al. [15], Ozoe et al. [16], Markatos and Pericleous [17], Afrid and Zebib [18] and Henkes and Hoogendoorn [19]. The difficulty of computation of turbulent natural convection by the conventional k–ε model with wall function method is the validity of the wall functions, which are based on the local equilibrium logarithmic velocity and temperature assumptions. The logarithmic wall functions were originally derived for the forced convection flows and do not hold for natural convection boundary layers. Due to this problem, many previous authors used the low-Reynolds-number turbulence models for the computation of natural convection problems, for example, Henkes et al. [20], Heindel et al. [21], Cha and Hsu [22], Sharif and Liu [23], Davidson [24], Inagaki and Komori [25] and Hsieh and Lien [26]. The works using the k–ω model have been done by Peng and Davidson [27] and Aounallah et al. [28].

The other difficulty in predicting the turbulent natural convection is the treatment of the turbulent heat fluxes. If one does not use the differential heat flux model, a proper way of treating the turbulent heat fluxes should be sought. All of the works reported above ([15–28]) used a simple gradient diffusion hypothesis (SGDH hereafter) in treating the turbulent heat fluxes. Ince and Launder [29] explained that the SGDH is not a proper way of treating the turbulent heat fluxes and proposed a generalized gradient diffusion hypothesis (GGDH hereafter). However, Kenjeres [30] has shown that the algebraic flux model (AFM hereafter) developed by Kenjeres and Hanjalic [31] results in better solutions than the GGDH for a stratified turbulent natural convection in enclosures. A good feature of the AFM developed by Kenjeres and Hanjalic [31] is its simplicity, it requires only one additional solution of the transport equation for a temperature variance. The main difference between the AFM and the GGDH is the inclusion of the temperature variance term in the algebraic expression of the turbulent heat fluxes. The use of the algebraic heat flux model is attractive due to its simplicity of implementation and high performance. The algebraic flux model was used by Kenjeres [30], Choi et al. [32] and by Liu and Wen [33]. Liu and Wen [33] included the damping functions and wall reflection terms in the algebraic representation of the turbulent heat fluxes, however, their solutions of the mean temperature and vertical velocity are not better than those by Kenjeres [30] or Choi et al. [32] who used the much simpler algebraic heat flux model by Kenjeres and Hanjalic [31].

It can be commonly accepted that the use of the second-moment closure may result in better solutions for natural convections in enclosures, however, the second-moment modeling of a natural convection requires the modeling of various terms in the transport equations for the turbulent heat flux vector, the temperature variance and the dissipation rate of the temperature variance, and its use in practical engineering problems is still questionable due to its complexity and demand of high computer resources. The near wall second-moment closures applied to the analysis of the turbulent natural convection in enclosures are rarely seen in the literatures and the examples using the second-moment closure are the works by Peeters and Henkes [34], Dol and Hanjalic [35] and Choi et al. [36].

It is also noted that the implementation of the wall reflection terms in the general purpose code that can handle the complex geometries is very difficult. This difficulty is due to the existence of wall related parameters such as the wall normal vector and the wall shear stress at the nearest wall from the calculation point, and the difficulty is not due to the solution method for the transport equations for the Reynolds stresses or turbulent heat fluxes. If the wall related parameters are included in the algebraic expression of the turbulent heat fluxes or Reynolds stresses, there is no advantage in introducing the algebraic stress model or AFM over the differential stress and flux model. The turbulence model free from the wall related parameters is the elliptic-blending model by Thielen et al. [37]. Recently Choi and Kim [38] obtained numerical solutions for a natural convection in an 1:5 rectangular cavity experimented by King [2] using the elliptic-blending model (EBM hereafter) by Thielen et al. [37], and showed that the solution by the EBM is superior to those by the two-equation models. It may be due to the fact that the EBM accurately calculates the Reynolds stresses when compared with the two-equation models which does not. Shin et al. [39] developed a differential flux model (DFM hereafter) with the EBM where the differential equations are solved for the turbulent heat fluxes.

The primary objective of the present study is to evaluate the GGDH, AFM and DFM with the EBM for the natural convection flows in rectangular and square cavities with different Rayleigh numbers. The experimental data used to evaluate the turbulence models are those by King [2] for an 1:5 rectangular cavity ($Ra = 4.3 \times 10^{10}$) and those by Ampofo and Karayiannis [6] for a square cavity with conducting walls ($Ra = 1.58 \times 10^{9}$). Peng and Davidson [7] performed an LES for the experiment by Ampofo and Karayiannis [6]. Even though the Rayleigh number differs by one order of a magnitude only, the flow features are quite different. The flow is a simple shear dominant flow in the experiment by King [2], however, in the experiment by Ampofo and Karayiannis [6] the boundary layer is thin

and about 90% of the flow is stagnant and stratified. Thus, the experiment by Ampofo and Karayiannis [6] may provide a critical experimental data for an evaluation of turbulence models. In the present study the mathematical formulation for each treatment is presented and the calculated results are compared with the experimental data to evaluate each treatment of the turbulent heat fluxes.

2. Governing equations

The ensemble-averaged governing equations for a conservation of the mass, momentum, energy and turbulent quantities for the elliptic-blending second-moment closure by Thielen et al. [37] can be written as follows:

$$\frac{\mathrm{D}}{\mathrm{D}t}(\rho) = 0 \tag{1}$$

$$\frac{\mathrm{D}}{\mathrm{D}t}(\rho U_i) = -\frac{\partial p}{\partial x_i} + \frac{\partial}{\partial x_j}\left(\mu\frac{\partial U_i}{\partial x_j} - \rho\overline{u_i u_j}\right) - \rho\beta g_i(\Theta - \Theta_{\mathrm{ref}}) \tag{2}$$

$$\frac{\mathrm{D}}{\mathrm{D}t}(\rho\Theta) = \frac{\partial}{\partial x_j}\left(\frac{\mu}{\mathrm{Pr}}\frac{\partial\Theta}{\partial x_j} - \rho\overline{\theta u_j}\right) \tag{3}$$

$$\frac{\mathrm{D}}{\mathrm{D}t}(\rho\overline{u_i u_j}) = \frac{\partial}{\partial x_k}\left[(\mu\delta_{kl} + C_s\rho\overline{u_k u_l}T)\frac{\partial\overline{u_i u_j}}{\partial x_l}\right] + \rho\left(P_{ij} + G_{ij} + \Phi_{ij} - \varepsilon_{ij}\right) \tag{4}$$

$$\frac{\mathrm{D}}{\mathrm{D}t}(\rho\varepsilon) = \frac{\partial}{\partial x_k}\left[(\mu\delta_{kl} + C_\varepsilon\rho\overline{u_k u_l}T)\frac{\partial\varepsilon}{\partial x_l}\right] + \frac{\rho(C_{\varepsilon1}(P_k + G_k) - C_{\varepsilon2}\varepsilon)}{T} \tag{5}$$

$$\frac{\mathrm{D}}{\mathrm{D}t}(\rho\overline{\theta^2}) = \frac{\partial}{\partial x_k}\left[\left(\frac{\mu}{\mathrm{Pr}}\delta_{kl} + C_{\theta\theta}\rho\overline{u_k u_l}T\right)\frac{\partial\overline{\theta^2}}{\partial x_l}\right] + \rho\left(2P_\theta - R\frac{\varepsilon}{k}\overline{\theta^2}\right) \tag{6}$$

$$\alpha - L^2\frac{\partial^2\alpha}{\partial x_j\partial x_j} = 1 \tag{7}$$

where

$$P_{ij} = -\overline{u_i u_k}\frac{\partial U_j}{\partial x_k} - \overline{u_j u_k}\frac{\partial U_i}{\partial x_k},$$

$$G_{ij} = -g_i\beta\overline{u_j\theta} - g_j\beta\overline{u_i\theta}, \quad P_\theta = -\overline{u_k\theta}\frac{\partial\Theta}{\partial x_k} \tag{8}$$

$$\Phi_{ij} = (1-\alpha^2)\Phi^w_{ij} + \alpha^2\Phi^h_{ij} \tag{9}$$

$$\Phi^h_{ij} = -\left(C_1 + C_2\frac{P_k}{\varepsilon}\right)\varepsilon A_{ij} + C_3 kS_{ij} + C_4 k\left(A_{ik}S_{jk} + A_{jk}S_{ik} - \frac{2}{3}\delta_{ij}A_{lk}S_{kl}\right) + C_5 k\left(A_{ik}\Omega_{jk} + A_{jk}\Omega_{ik}\right) - C_6\left(G_{ij} - \frac{2}{3}G_K\delta_{ij}\right) \tag{10}$$

$$\Phi^w_{ij} = -5\frac{\varepsilon}{k}\left(\overline{u_i u_k}n_j n_k + \overline{u_j u_k}n_i n_k - \frac{1}{2}C_1\overline{u_k u_l}n_k n_l\left(n_i n_j + \delta_{ij}\right)\right) \tag{11}$$

$$\varepsilon_{ij} = (1-\alpha^2)\frac{\overline{u_i u_j}}{k}\varepsilon + \frac{2}{3}\alpha^2\varepsilon\delta_{ij} \tag{12}$$

$$n = \frac{\nabla\alpha}{\|\nabla\alpha\|}, \quad A_{ij} = \frac{\overline{u_i u_j}}{k} - \frac{2}{3}\delta_{ij},$$
$$S_{ij} = \frac{1}{2}\left(\frac{\partial U_i}{\partial x_j} + \frac{\partial U_j}{\partial x_i}\right), \quad \Omega_{ij} = \frac{1}{2}\left(\frac{\partial U_i}{\partial x_j} - \frac{\partial U_j}{\partial x_i}\right) \tag{13}$$

$$T = \max\left(\frac{k}{\varepsilon}, C_T\left(\frac{\nu}{\varepsilon}\right)^{1/2}\right),$$
$$L = C_L\max\left(\frac{k^{3/2}}{\varepsilon}, C_\eta\left(\frac{\nu^3}{\varepsilon}\right)^{1/4}\right) \tag{14}$$

and

$$C_S = 0.21, \quad C_\varepsilon = 0.18, \quad C^0_{\varepsilon1} = 1.44, \quad C_{\varepsilon2} = 1.83, \quad C_{\theta\theta} = 0.22, \quad R = 2. \tag{15}$$

$$C_1 = 1.7, \quad C_2 = 0.9, \quad C_3 = 0.8 - 0.65A_2^{1/2}, \quad C_4 = 0.62, \quad C_5 = 0.2, \quad C_6 = 0.3 \tag{16}$$

$$C_T = 6.0, \quad C_L = 0.161, \quad C_\eta = 80. \tag{17}$$

$$C_{\varepsilon1} = C^0_{\varepsilon1}\left(1 + 0.03(1-\alpha^2)\sqrt{\frac{k}{\overline{u_i u_j}n_i n_j}}\right) \tag{18}$$

3. Treatment of turbulent heat fluxes

3.1. Simple gradient diffusion hypothesis (SGDH)

In the SGDH, the turbulent heat fluxes ($\overline{\theta u_j}$) in Eq. (3) are treated by the following equation.

$$\overline{\theta u_i} = -\frac{\nu_t}{Pr_t}\frac{\partial\Theta}{\partial x_i}, \quad \nu_t = C_\mu\frac{k^2}{\varepsilon} \tag{19}$$

In this equation, $Pr_t = 0.9$ is the turbulent Prandtl number and $C_\mu = 0.09$. It is well known that this assumption is not adequate for a natural convection even though it is used widely for forced convection flows. Thus, this assumption is not employed in the present study. Interested readers can refer to Kenjeres et al. [40] for its performance for a natural convection with the elliptic relaxation model.

3.2. Generalized gradient diffusion hypothesis (GGDH)

In the GGDH, the turbulent heat fluxes ($\overline{\theta u_j}$) in Eq. (3) are given by the following equation.

$$\overline{\theta u_i} = -C_\theta\frac{k}{\varepsilon}\left(\overline{u_i u_k}\frac{\partial\Theta}{\partial x_k}\right) \tag{20}$$

The value of the constant, $C_\theta = 0.3$, is given in Thielen et al. [37]. As shown in the above equation, the accuracy

of this assumption depends on the accuracy of the computed Reynolds stresses. For a natural convection, Ince and Launder [29] and Choi and Kim [38] used the GGDH and it is well known that this assumption is not adequate for a natural convection with a strong stratification.

3.3. Algebraic flux model (AFM)

In the AFM the turbulent heat fluxes are computed by the following algebraic equation:

$$\overline{\theta u_i} = -C_\theta \frac{k}{\varepsilon}\left(\overline{u_i u_j}\frac{\partial \Theta}{\partial x_j} + \xi\overline{\theta u_j}\frac{\partial U_i}{\partial x_j} + \eta\beta g_i\overline{\theta^2}\right) \tag{21}$$

In the present study the values of the constants are given as $C_\theta = 0.2$, $\eta = 0.6$, $\xi = 0.6$. When compared with the GGDH model, the last term with a temperature variance has a positive effect on G_k and it prevents G_k from being too negative a value. This effect stabilizes the overall solution process, especially for strongly stratified flows.

3.4. Differential flux model (DFM)

Shin et al. [39] proposed the following differential equations for the turbulent heat fluxes.

$$\frac{\mathrm{D}}{\mathrm{D}t}(\rho\overline{u_i\theta}) = \frac{\partial}{\partial x_k}\left[\left(\frac{1}{2}(\mu + \frac{\mu}{\mathrm{Pr}})\delta_{kl} + C_\theta\rho\overline{u_k u_l}T\right)\frac{\partial\overline{u_i\theta}}{\partial x_l}\right] + \rho(P_{i\theta} + G_{i\theta} + \Phi^*_{i\theta} - \varepsilon_{i\theta}) \tag{22}$$

where

$$P_{i\theta} = -\overline{u_i u_k}\frac{\partial\Theta}{\partial x_k} - \overline{u_k\theta}\frac{\partial U_i}{\partial x_k} \tag{23}$$

$$G_{i\theta} = -g_i\beta\overline{\theta^2} \tag{24}$$

$$\Phi^*_{i\theta} = (1-\alpha^2)\Phi^w_{i\theta} + \alpha^2\Phi^h_{i\theta} \tag{25}$$

$$\varepsilon_{i\theta} = (1-\alpha^2)\varepsilon^w_{i\theta} + \alpha^2\varepsilon^h_{i\theta} \tag{26}$$

$$\Phi^h_{i\theta} = -C_{1\theta}\frac{\varepsilon}{k}\overline{u_i\theta} + C_{2\theta}\overline{u_j\theta}\frac{\partial U_i}{\partial x_j} + C_{3\theta}g_i\beta\overline{\theta^2} \tag{27}$$

$$\Phi^w_{i\theta} = -\frac{\varepsilon}{k}\overline{u_k\theta}n_k n_i \tag{28}$$

$$\varepsilon^h_{i\theta} = 0, \quad \varepsilon^w_{i\theta} = \frac{1}{2}\left(1 + \frac{1}{\mathrm{Pr}}\right)\frac{\varepsilon}{k}(\overline{u_i\theta} + \overline{u_k\theta}n_k n_i) \tag{29}$$

$$C_{1\theta} = 3.75, \quad C_{2\theta} = 0.5, \quad C_{3\theta} = 0.5 \tag{30}$$

This model has not been tested for natural convection flows and thus it will be tested in the present study.

4. Adjustment of turbulence model constants

The original EBM by Thielen et al. [37] has been used for the calculation of the King's experiment by Choi and Kim [38]. In this study only the model constant C_L has been changed from $C_L = 0.161$ to $C_L = 0.145$. According to our numerical experiment, the model constants in Thielen et al. [37] only work well for the GGDH. However, it does not produce accurate solutions with the AFM and DFM, and thus, an adjustment of the constants in the EBM by Thielen et al. [37] has been performed through several numerical calculations. The following constants are adjusted for the AFM and DFM.

$$C_{\varepsilon 1} = 1.44\left(1 + 0.1\frac{(P_k + G_k)}{\varepsilon}\right), \quad C_{\varepsilon 2} = 1.92,$$
$$C_\eta = 50. \tag{31}$$

We also adjusted the constant, C_L, and it was dependent on the flow conditions and turbulence models. For King's experiment it was $C_L = 0.13$ for the AFM and $C_L = 0.15$ for the DFM. For Ampofo's experiment it was $C_L = 0.16$ for the AFM and $C_L = 0.18$ for the DFM. It is worth while mentioning here that we could not obtain an accurate solution when we used the $C_{\varepsilon 1}$ by Eq. (18) for the AFM and the DFM, and the Eq. (18) only works well for the GGDH.

5. Boundary conditions

For the boundary conditions at the wall, a no slip boundary condition is imposed for the velocity components and isothermal and adiabatic wall boundary conditions are imposed for the temperature. The Reynolds stresses and the temperature variance are zero at the wall.

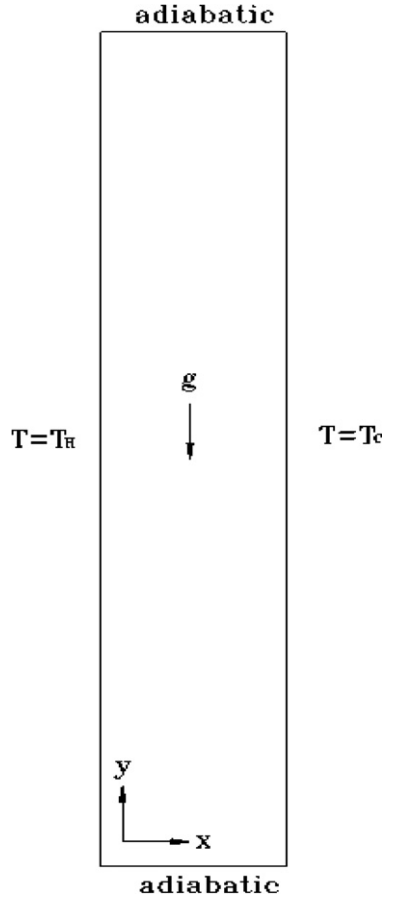

Fig. 1. A schematic picture of the 5:1 rectangular cavity.

$$U_w = V_w = 0, \quad \overline{uu_w} = \overline{vv_w} = \overline{ww_w} = \overline{uv_w} = 0, \quad \overline{\theta_w^2} = 0,$$
$$\alpha_w = 0, \quad \varepsilon_w = 2\nu\frac{k}{y^2} \tag{32}$$

$$\Theta(x=0) = \Theta_{\text{hot}}, \quad \Theta(x=L) = \Theta_{\text{cold}},$$
$$\frac{\partial\Theta}{\partial y}(y=0,H) = 0 (\text{or} \Theta(y=0,H) : \text{ specified}) \tag{33}$$

6. Numerical methods

The turbulence models considered in the present study are implemented in the computer code especially designed for the evaluation of turbulence models. The computer code employs the non-staggered grid arrangement and the SIMPLE algorithm by Patankar [41] for the pressure–velocity coupling. The second-order bounded HLPA scheme by Zhu [42], which is the same as the Van-Leer's CLAM scheme [43], is used for treating the convection terms for all the computed variables.

7. Results and discussion

7.1. Natural convection in a rectangular cavity

The first test problem considered in the present study is a natural convection of air in a rectangular cavity with an aspect ratio of 1:5 as shown in Fig. 1. The height of the cavity is $H = 2.5$ m, the width of the cavity is $L = 0.5$ m and the temperature difference between the hot and cold walls

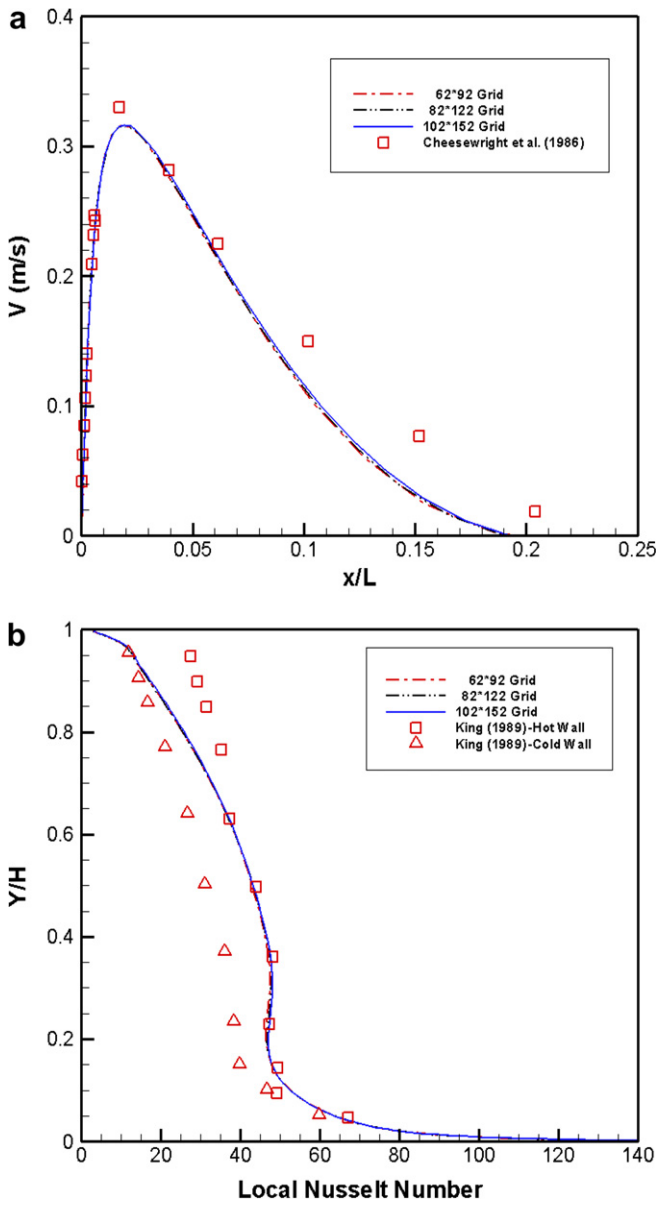

Fig. 2. Grid independency test for the King's experiment, (a) vertical velocity profiles at $y/H = 0.5$, (b) local Nusselt number profiles at hot wall.

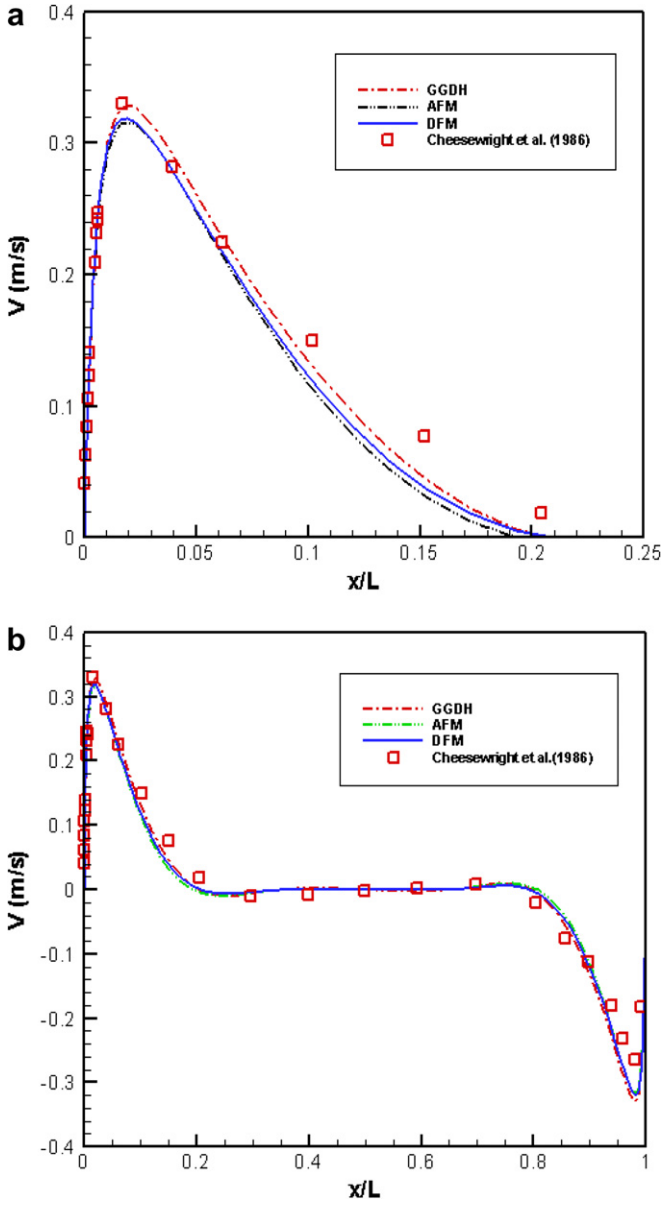

Fig. 3. Mean vertical velocity profiles at $y/H = 0.5$, (a) near the hot wall, (b) total view.

is 45.8 °K. The Rayleigh number based on the height of the cavity is $Ra = 4.3 \times 10^{10}$ and the Prandtl number is $Pr = 0.71$. King [2] has carried out extensive measurements for this problem and his experimental data is reported in King [2] and Cheesewright et al. [3]. The experimental data by King [2] contains a problem in that the top wall is not fully insulated. This makes the turbulence level near the hot wall high and that near the cold wall low, and this affects the distribution of the turbulence quantities in all the solution domain. Such a deficiency will be shown clearly for the distribution of the Reynolds shear stress at $y/H = 0.5$. However, it is not easy to avoid such an experimental difficulty. In order to check the grid independency of the solution, calculations are performed using three different grids, 62×92, 82×102 and 102×152. Fig. 2 shows that the present solutions are grid independent. The solution given in the following plots are that by the finer grid (102×152). The first grid point from the wall is $x^+ = 0.1$ for all AFM, DFM and GGDH models.

We first compared the predicted results with the measured data reported in Cheesewright et al. [3] for the vertical mean velocity at a mid-height ($y/H = 0.5$) of the cavity. Fig. 3 show the comparison of the predicted results with the measured data for the vertical velocity component at $y/H = 0.5$. As shown in the figures, the agreement between the measured data and the predictions by the GGDH, AFM and DFM models are fairly good although a small difference exists. The GGDH solution here is that by Choi and Kim [38]. This figure shows that the GGDH model

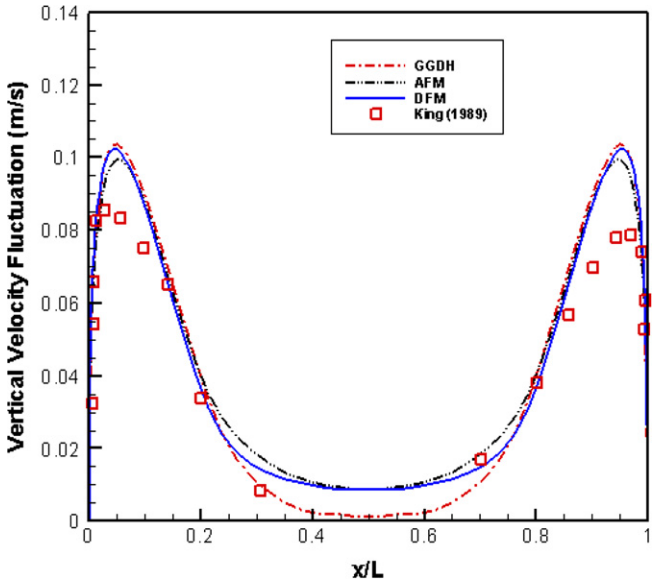

Fig. 4. Vertical velocity fluctuation profiles at $y/H = 0.5$.

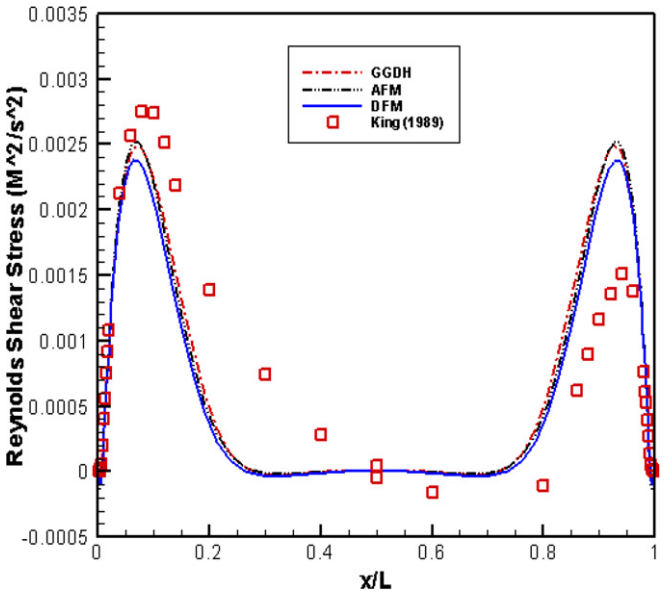

Fig. 5. Reynolds shear stress profiles at $y/H = 0.5$.

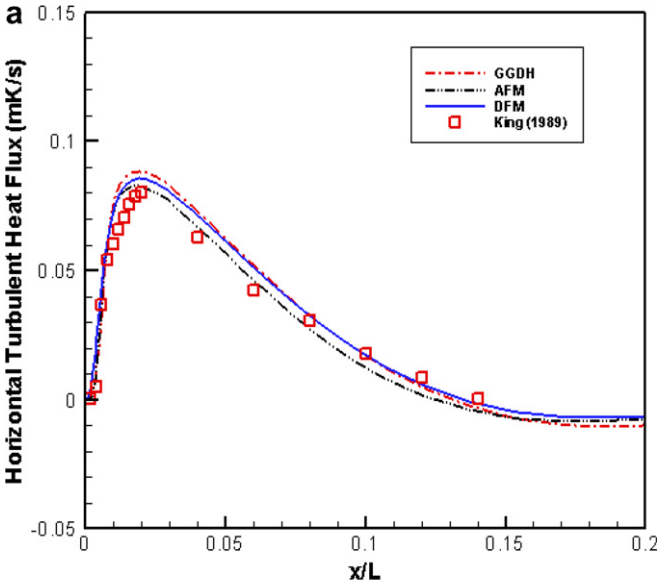

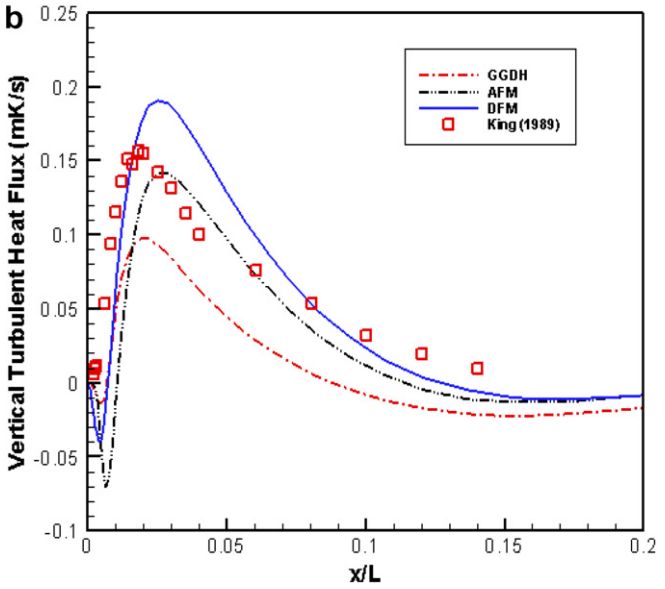

Fig. 6. Turbulent heat fluxes profiles at $y/H = 0.5$, (a) horizontal turbulent heat flux $\overline{\theta u}$, (b) vertical turbulent heat flux $\overline{\theta v}$.

predicts the mean vertical velocity fairly well for this simple shear dominant flow without a strong stratification.

Fig. 4 shows the comparison of the predicted vertical velocity fluctuation at a mid-height ($y/H = 0.5$) with the experimental data. The GGDH, AFM and DFM over-predict it in the near wall region. The experimental data shows a symmetric profile, however, when one considers the insufficient insulation problem at the top wall, the profile near the hot wall is not a correct one. Therefore, the magnitude of the experimental data near the hot wall should be greater than that near the cold wall. We observed that the predictions follow the trend of the measured data well except for the central region of the cavity where the flow is weakly stratified. The prediction by GGDH shows that the vertical velocity fluctuation is nearly zero at the central region of the cavity even in this weakly stratified region, while AFM and DFM avoid this problem. As mentioned before, it is due to the fact that a gravity term with a temperature variance exists in the algebraic (AFM) or differential (DFM) formulations of the turbulent heat fluxes. We can conjecture that the GGDH model may invoke a numerical stability problem when it is applied to flows with a strong stratification. Fig. 5 shows the profiles of the predicted Reynolds shear stress $\overline{uv}$ at a mid-plane ($y/H = 0.5$) of the cavity together with the measured data. The GGDH, AFM and DFM models slightly under-predict the $\overline{uv}$ near the hot wall and over-predict it near the cold wall due to the insufficient insulation problem at the top wall. The performances of the three models for the prediction of $\overline{uv}$ are nearly the same.

Fig. 6 shows the profiles of the predicted horizontal and vertical turbulent heat fluxes, $\overline{\theta v}$ and $\overline{\theta u}$, at a mid-plane ($y/H = 0.5$) of the cavity with the measured data. It is noted that the vertical turbulent heat flux vector $\overline{\theta v}$ plays a very important role in the dynamics of the turbulent kinetic energy in the buoyant turbulent flows and it directly influences the overall prediction of all the quantities. It is noted that the AFM and DFM contain all the temperature and mean velocity gradients together with a correlation between the gravity vector and temperature variance. The three models predict the horizontal turbulent heat flux $\overline{\theta u}$ fairly well. The GGDH model under-predicts the vertical turbulent heat flux $\overline{\theta v}$ near the hot wall while the DFM slightly over-predicts it. The AFM predicts best the vertical turbulent heat flux near the hot wall region.

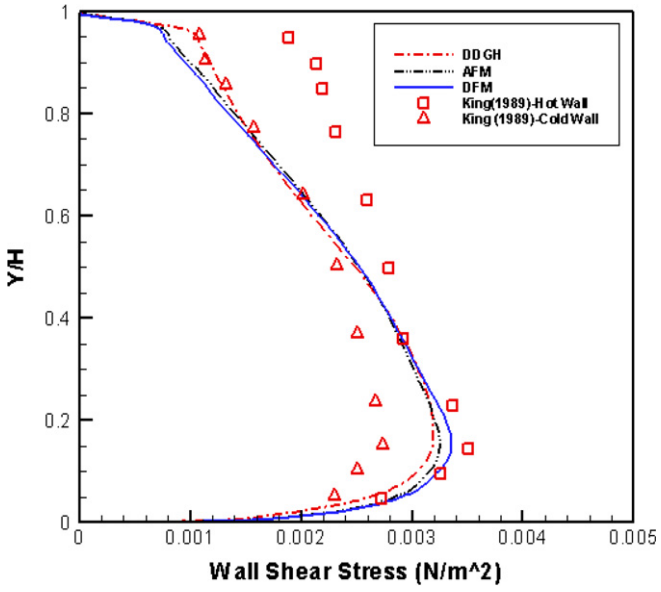

Fig. 7. Wall shear stress distribution along the vertical wall.

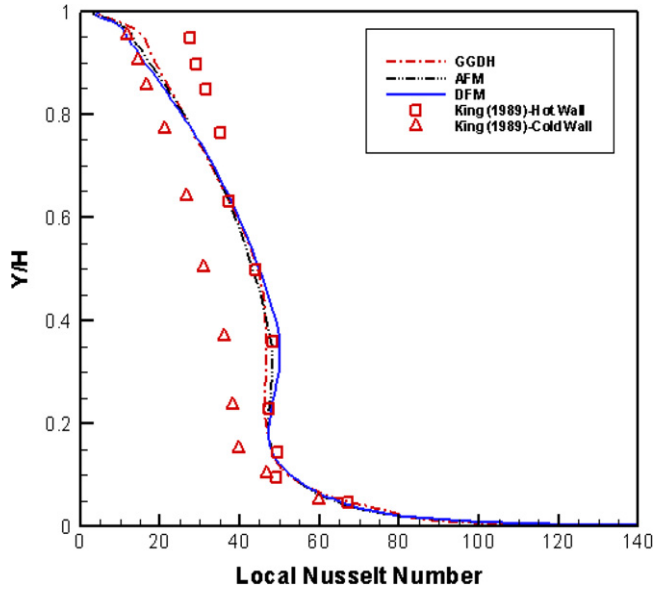

Fig. 8. Local Nusselt number distribution along the vertical wall.

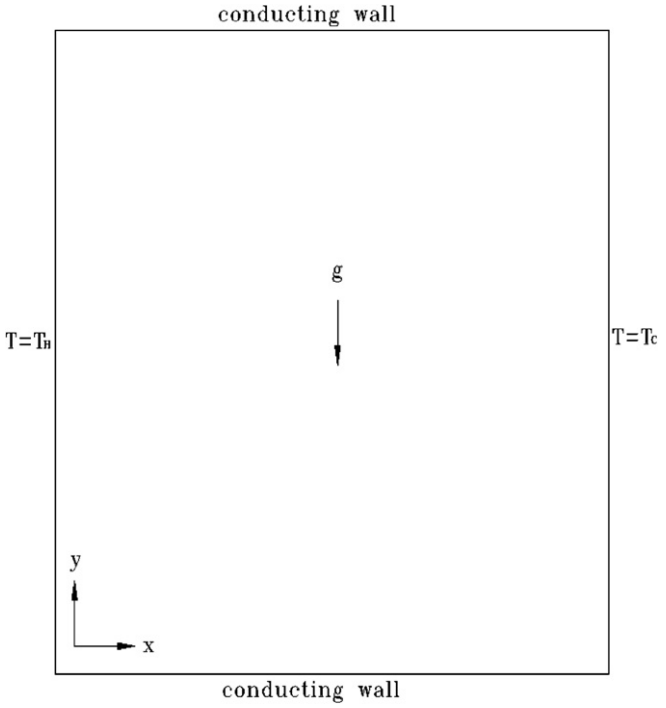

Fig. 9. A schematic picture of the square cavity with conducting walls.

Figs. 7 and 8 show the comparisons of the predicted results with the measured data for the wall shear stress and the local Nusselt number at the hot wall reported in King [2]. The three models predict the wall shear stress and local Nusselt number at the hot wall very well and the smooth laminar to turbulent transition at the lower portion of the hot wall observed in the experimental data is also predicted well.

7.2. Natural convection in a square cavity with conducting walls

The second test problem is the experiment conducted by Ampofo and Karayiannis [6]. This test problem is a natural convection of air in a square cavity with two isothermal side walls and two conducting walls at the top and bottom as shown in Fig. 9. The height of the cavity is $H = 0.75$ m and the temperature difference between the hot and cold walls is 40 °K. The Rayleigh number based on the height of the cavity is $Ra = 1.58 \times 10^9$ and the Prandtl number is $Pr = 0.71$. The detailed experimental data is tabulated in Ampofo and Karayinnis [6]. The top and bottom walls are conducting walls and the boundary conditions for the temperature for these walls are specified by using the data given in Ampofo and Karayinnis [6]. The experiment conducted by Ampofo and Karayiannis [6] for a square cavity is the most challenging case for an evaluation of turbulence models. The turbulence level in the central region is very low, and the flow is stagnant and thermally stratified. The boundary layer is thin and the turbulence intensity level is low. The LES solution by Peng and Davidson [7] is available for this flow and it is compared with the present

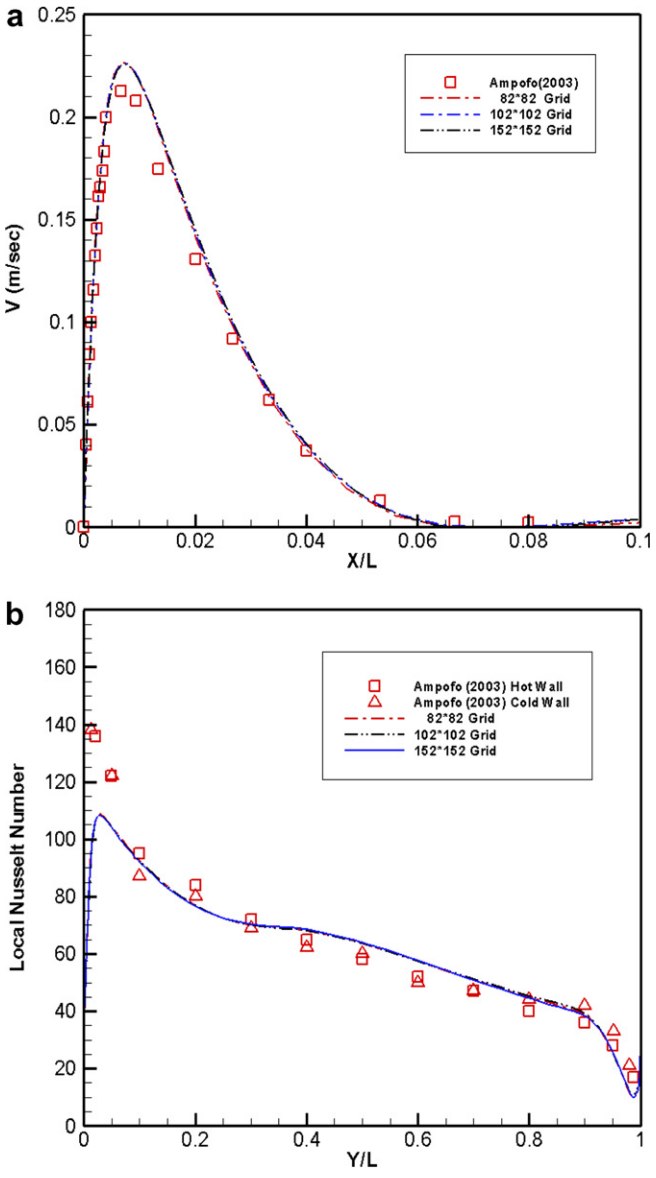

Fig. 10. Grid independency test for the Ampofo's experiment, (a) vertical velocity profiles at $y/H = 0.5$, (b) local Nusselt number profiles at hot wall.

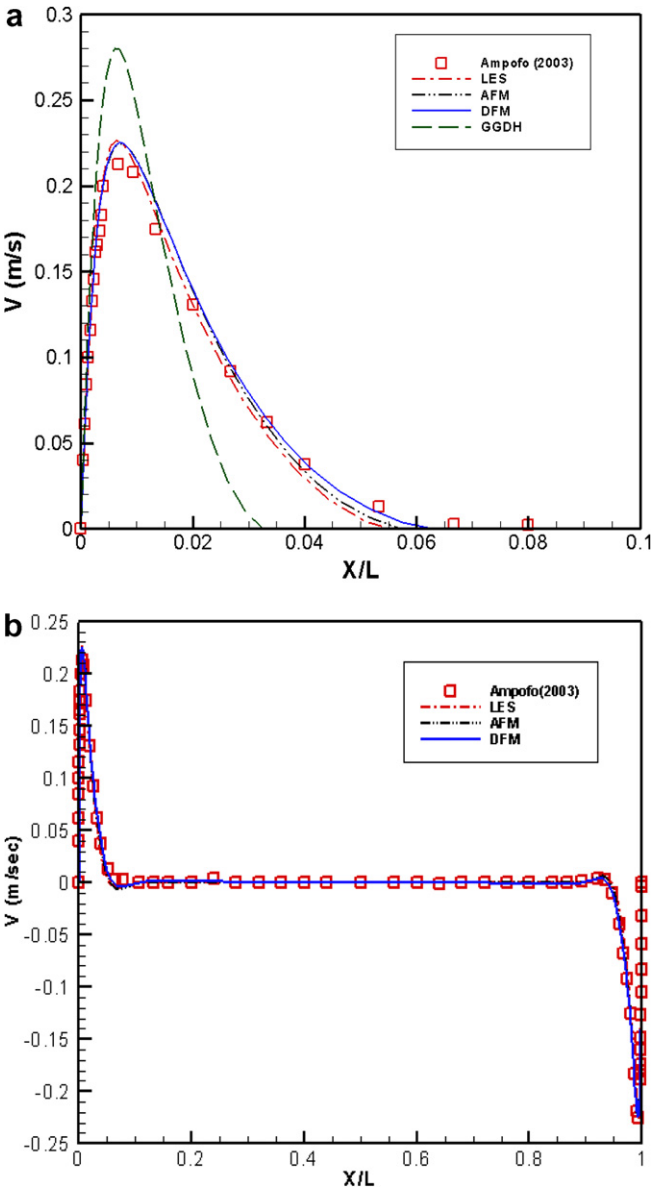

Fig. 11. Mean vertical velocity profiles at $y/H = 0.5$, (a) near the hot wall, (b) total view.

predictions. The subgrid-scale model used in this calculation is the Smagorinsky model [44] incorporated into dynamic procedure. The grid independency of solutions is also checked for this flow. Calculations are performed using three different grids, 82×82, 102×102 and 152×152. Fig. 10 shows that the present solutions are grid independent. The first grid point from the wall is $x^+ = 0.135$ for both AFM and DFM models.

We first compared the predicted results with the measured data reported in Ampofo and Karayinnis [6] for the vertical mean velocity. Fig. 11 show the comparisons of the predicted results with the measured data for the vertical velocity component at a mid-height ($y/H = 0.5$) of the cavity. As shown in the figure, the agreement between the measured data and the predictions by the AFM and DFM models is very good and follows the trend of the measured data. However, we can observe that the solution by the GGDH model looks like laminar solution and deviates much from the experimental data. As shown before, Choi and Kim [38] predicts accurate solutions for a simple shear dominant flow within the 1:5 rectangular cavity using the GGDH model, however, this model predicts a very poor solution or invokes a numerical oscillation when applied to a flow with a relatively strong stratification like the present problem. Due to this reason we did not perform an adjustment of the turbulence model constants for the GGDH for this problem. We can observe that the predictions by the AFM and DFM turbulence models are as good as the LES solution.

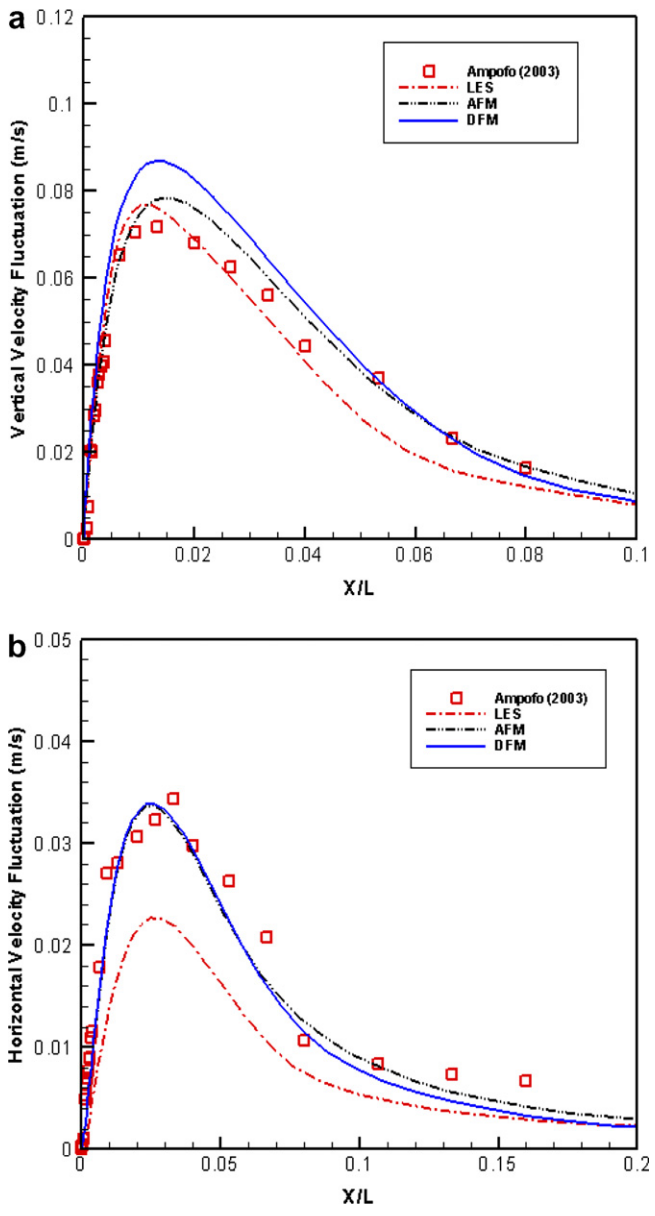

Fig. 12. Vertical and horizontal velocity fluctuation profiles at $y/H = 0.5$, (a) vertical velocity fluctuation, (b) horizontal velocity fluctuation.

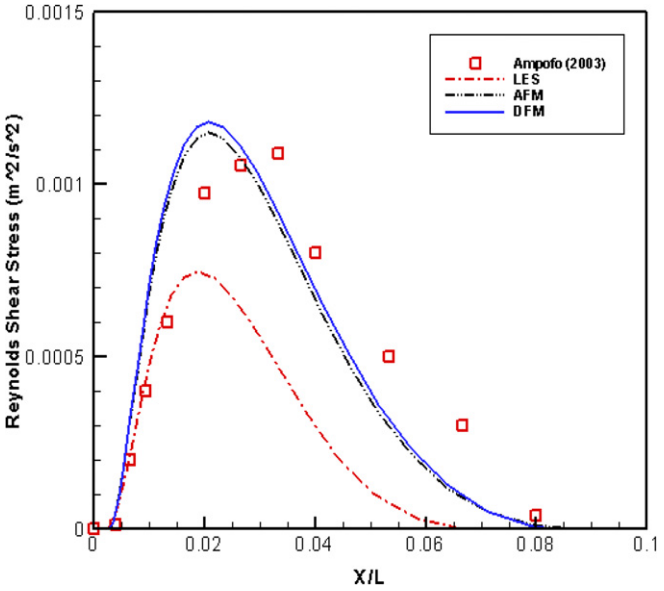

Fig. 13. Reynolds shear stress $\overline{uv}$ profiles at $y/H = 0.5$.

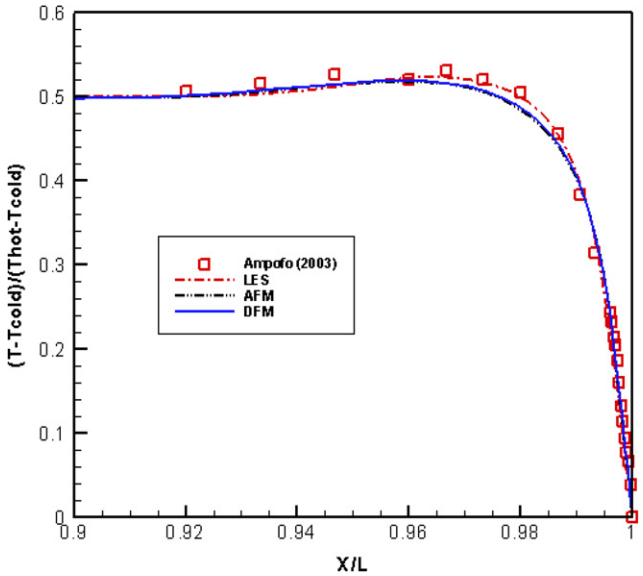

Fig. 14. Horizontal centerline temperature profiles at $y/H = 0.5$.

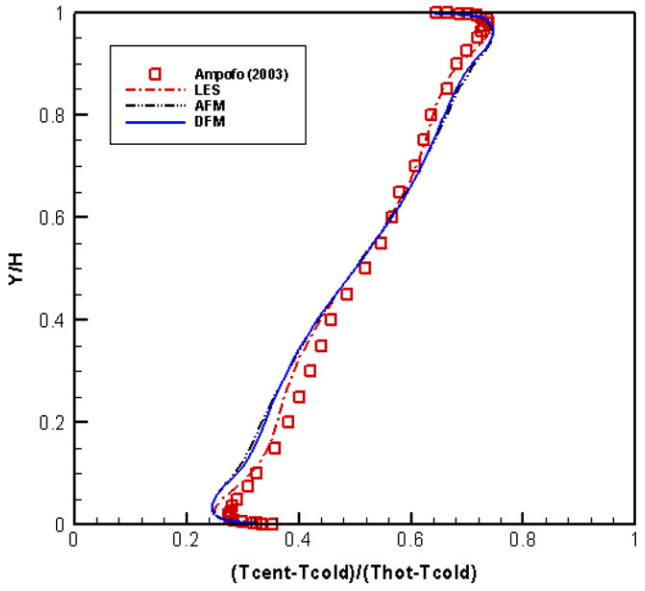

Fig. 15. Vertical centerline temperature profiles at $x/L = 0.5$.

Figs. 12 and 13 show the comparisons of the predicted results with the measured data for the turbulent quantities such as the horizontal and vertical velocity fluctuations and the Reynolds shear stress at a vertical mid-plane of the cavity ($y/H = 0.5$). Figs. 12 and 13 show that the predictions by the AFM and DFM agree well with the measured data although the DFM slightly over-predicts the vertical velocity fluctuation. It is not understood why the LES calculation by Peng and Davidson [7] under-predicts the turbulent quantities.

Figs. 14 and 15 show the comparisons of the predicted results with the measured data for the mean temperature at a mid-height ($y/H = 0.5$) and at a mid-width ($x/L = 0.5$) of the cavity. No real differences among the models for the horizontal temperature distribution at a mid-plane ($y/H = 0.5$) exist. In the vertical direction, the AFM and DFM models slightly under-predict it near the bottom wall and over-predict it near the top wall, while the LES predicts it accurately.

Fig. 16 shows the predicted results for the local Nusselt number at the hot and bottom walls together with the measured data. It is observed that the DFM model slightly over-predicts the local Nusselt number at the hot and bottom walls, while the AFM rather accurately predicts the local Nusselt number at the hot and bottom walls. It is noted that the predictions of the local Nusselt number at the hot wall by the AFM and DFM show a smooth transition which was not observed in the experimental data and LES solution. The AFM predicts the Nusselt number as accurately as the LES solution.

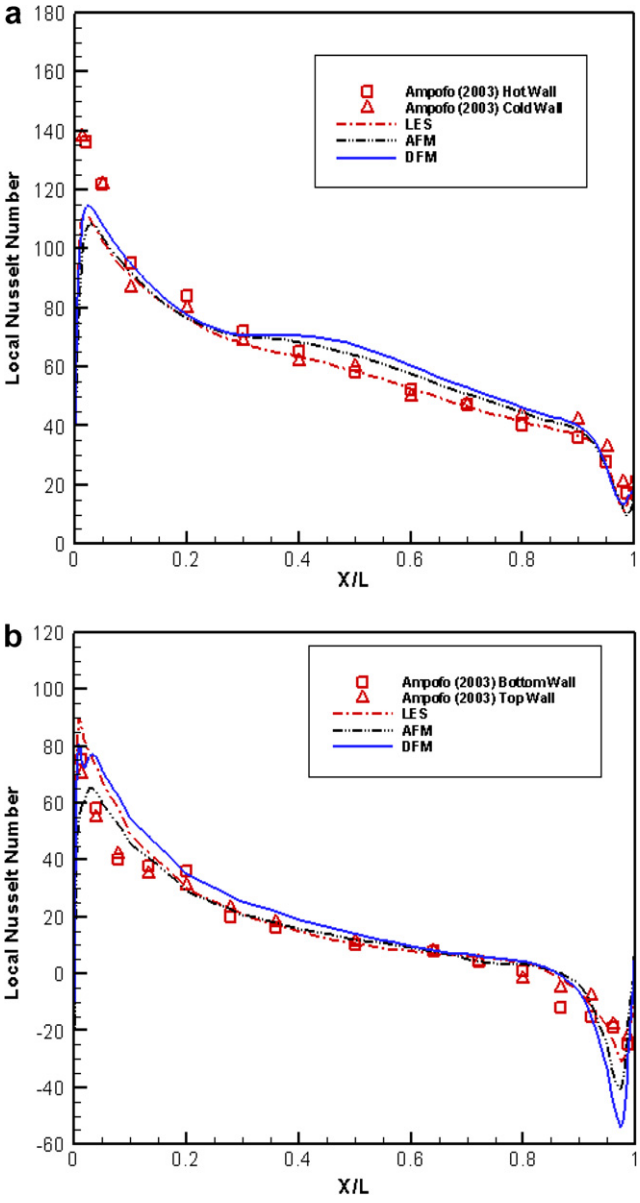

Fig. 16. Local Nusselt number distributions along the hot and bottom walls, (a) hot wall, (b) bottom wall.

8. Conclusions

The treatment of turbulent heat fluxes with the EBM is tested for a turbulent natural convection in a rectangular cavity and in a square cavity with different geometries and Rayleigh numbers. The performances of the turbulence models are investigated through comparisons with the available experimental data. The following conclusions are drawn from the present study:

(1) In general the performances of the AFM and DFM for a prediction of the mean vertical velocity component and temperature, thereby the wall shear stress and the Nusselt number, were similar, and the vertical turbulent quantities were slightly better predicted by the AFM. Since the DFM needs computation of two more transport equations for the turbulent heat fluxes in the two-dimensional situation, the DFM needs a more computational time even though it is not so grave. The more important problem is that a

more accurate modeling of transport equations for turbulent heat fluxes is needed. Thus, the AFM is a better choice at the present time, especially in the three-dimensional situation.

(2) The GGDH only predicts an accurate solution for a simple shear dominant flow, however, the model predicts very poor solutions or invokes a numerical oscillation when applied to a flow with a strong stratification.

(3) The LES predicts the mean vertical velocity component and temperature, thereby the Nusselt number, better than the AFM and DFM. However, it predicts a poor solution for the turbulent quantities. This discrepancy is not clearly understood at present.

When one considers the fact that the wall related parameters, which hinder an implementation of the models in the general purpose commercial codes, do not exist in the EBM and its performance with the AFM or DFM is very good, the use of the EBM for a turbulent natural convection is highly recommended.

Acknowledgement

This study has been supported by the Nuclear Research and Development Program of the Ministry of Science and Technology of Korea. The authors would like to acknowledge support from the Korea Institute of Science and Technology Information under the eighth Strategic Supercomputing Support Program with S.M. Lee as the technical supporter. The use of the computing system of the Supercomputing Center is also greatly appreciated.

References

[1] T. Tsuji, Y. Nagano, Turbulence measurements in a natural convection boundary layer along a vertical flat plate, Int. J. Heat Mass Transfer 31 (1987) 2101–2111.

[2] K.V. King, Turbulent natural convection in rectangular air cavities, Ph.D Thesis, Queen Mary College, University of London, UK, 1989.

[3] R. Cheesewright, K.J. King, S. Ziai, Experimental data for the validation of computer codes for the prediction of two-dimensional buoyant cavity flows, Proceedings of ASME Meeting, HTD 60 (1986) 75–86.

[4] P.L. Betts, I.H. Bokhari, Experiments on turbulent natural convection in an enclosed tall cavity, Int. J. Heat Fluid Flow 21 (2000) 675–683.

[5] Y.S. Tian, T.G. Karayiannis, Low turbulence natural convection in an air filled square cavity part I: the thermal and fluid flow fields, Int. J. Heat Mass Transfer 43 (2000) 849–866.

[6] F. Ampofo, T.G. Karayiannis, Experimental benchmark data for turbulent natural convection in an air filled square cavity, Int. J. Heat Mass Transfer 46 (2003) 3551–3572.

[7] S.H. Peng, L. Davidson, Large eddy simulation of turbulent buoyant flow in a confined cavity, Int. J. Heat Fluid Flow 22 (2001) 323–331.

[8] Y.S. Tian, T.G. Karayiannis, Low turbulence natural convection in an air filled square cavity part II: the turbulence quantities, Int. J. Heat Mass Transfer 43 (2000) 867–884.

[9] S. Kenjeres, K. Hanjalic, LES, T-RANS and hybrid simulations of thermal convection at high Ra numbers, Int. J. Heat Fluid Flow 27 (2006) 800–810.

[10] R. Boudjemadi, V. Maupu, D. Laurence, P.Le. Quere, Budgets of turbulent stresses and fluxes in a vertical slot natural convection flow at Rayleigh $Ra = 10^5$ and 5.4×10^5, Int. J. Heat Fluid Flow 18 (1997) 70–79.

[11] T.A.M. Versteegh, F.T.M. Nieuwstat, Turbulence budgets of natural convection in an infinite, differentially heated, vertical wall, Int. J. Heat Fluid Flow 19 (1998) 135–149.

[12] M. Worner, G. Grotzbach, Pressure transport in direct numerical simulations of turbulent natural convection in horizontal fluid layers, Int. J. Heat Fluid Flow 19 (1998) 150–158.

[13] K. Hanjalic, One-point closure models for buoyancy-driven turbulent flows, Annu. Rev. Fluid Mech. 34 (2002) 321–347.

[14] H.S. Dol, K. Hanjalic, S. Kenjeres, A comparative assessment of the second-moment differential and algebraic models in turbulent natural convection, Int. J. Heat Fluid Flow 18 (1997) 4–14.

[15] R.A. Kuyper, TH.H. Van Der Meer, C.J. Hoogendoorn, R.A.W.M. Henkes, Numerical study of laminar and turbulent natural convection in an inclined square cavity, Int. J. Heat Mass Transfer 36 (1993) 2899–2911.

[16] H. Ozoe, A. Mouri, M. Ohmuro, S.W. Churchill, N. Lior, Numerical calculations of laminar and turbulent natural convection in water in rectangular channels heated and cooled isothermally on the opposing vertical walls, Int. J. Heat Mass Transfer 28 (1985) 125–138.

[17] N.C. Markatos, K.A. Pericleous, Laminar and turbulent natural convection in an enclosed cavity, Int. J. Heat Mass Transfer 27 (1984) 755–772.

[18] M. Afrid, A. Zebib, Three-dimensional laminar and turbulent natural convection cooling of heated blocks, Numer. Heat Transfer: Part A 19 (1991) 405–424.

[19] R.A.W.M. Henkes, C.J. Hoogendoorn, Comparison exercise for computations of turbulent natural convection in enclosures, Numer. Heat Transfer: Part B 28 (1995) 59–78.

[20] R.A.W.M. Henkes, F.F. Van Der Vlugt, C.J. Hoogendoorn, Natural-convection flow in a square cavity calculated with low-Reynolds-number turbulence models, Int. J. Heat Mass Transfer 34 (1991) 377–388.

[21] T.J. Heindel, S. Ramadhyani, F.P. Incropera, Assessment of turbulence models for natural convection in an enclosure, Numer. Heat Transfer: Part B 26 (1994) 147–172.

[22] M.I. Char, Y.H. Hsu, Comparative analysis of linear and nonlinear low-Reynolds-number eddy viscosity models to turbulent natural convection in horizontal cylindrical annuli, Numer. Heat Transfer: Part A 33 (1998) 191–206.

[23] M.A.R. Sharif, W. Liu, Numerical study of turbulent natural convection in a side-heated square cavity at various angles of inclination, Numer. Heat Transfer: Part A 43 (2003) 693–716.

[24] L. Davidson, Calculation of the turbulent buoyancy-driven flow in a rectangular cavity using an efficient solver and two different low Reynolds number k–ε turbulence models, Numer. Heat Transfer: Part A 18 (1990) 129–147.

[25] T. Inagaki, K. Komori, Numerical modeling on turbulent transport with combined forced and natural convection between two vertical parallel plates, Numer. Heat Transfer: Part A 27 (1995) 417–431.

[26] K.J. Hsieh, F.S. Lien, Numerical modeling of buoyancy-driven turbulent flows in enclosures, Int. J. Heat Fluid Flow 25 (2004) 659–670.

[27] S.H. Peng, L. Davidson, Computation of turbulent buoyant flows in enclosures with low-Reynolds-number k–ω models, Int. J. Heat Fluid Flow 20 (1999) 172–184.

[28] M. Aounallah, Y. Addad, S. Benhamadouche, O. Imine, L. Adjlout, D. Laurence, Numerical investigation of turbulent natura convection in an inclined square cavity with a hot wavy wall, Int. J. Heat Mass Transfer 50 (2007) 1683–1693.

[29] N.Z. Ince, B.E. Launder, On the computation of buoyancy-driven turbulent flows in rectangular enclosures, Int. J. Heat Fluid Flow 10 (1989) 110–117.

[30] S. Kenjeres, Numerical modeling of complex buoyancy-driven flows. Ph.D. Thesis, Delft University of Technology, The Netherlands, 1998.

[31] S. Kenjeres, K. Hanjalic, Prediction of turbulent thermal convection in concentric and eccentric annuli, Int. J. Heat Fluid Flow 16 (1995) 428–439.
[32] S.K. Choi, E.K. Kim, S.O. Kim, Computation of turbulent natural convection in a rectangular cavity with the k–ε–v^2–f model, Numer. Heat Transfer: Part B 45 (2004) 159–179.
[33] F. Liu, J.X. Wen, Development of and validation of an advanced turbulence model for buoyancy driven flows in enclosures, Int. J. Heat Mass Transfer 42 (1999) 3967–3981.
[34] T.W.J. Peeters, R.A.W.M. Henkes, The Reynolds-stress model of turbulence applied to the natural-convection boundary layer along a heated vertical plate, Int. J. Heat Mass Transfer 35 (1992) 403–420.
[35] H.S. Dol, K. Hanjalic, Computational study of turbulent natural convection in a side-heated near-cubic enclosure at a high Rayleigh number, Int. J. Heat Mass Transfer 44 (2001) 2323–2344.
[36] S.K. Choi, E.K. Kim, M.H. Wi, S.O. Kim, Computation of a turbulent natural convection in a rectangular cavity with the low-Reynolds-number differential stress and flux model, KSME Int. J. 18 (2004) 1782–1798.
[37] L. Thielen, K. Hanjalic, H. Jonker, R. Manceau, Prediction of flow and heat transfer in multiple Impinging jets with an elliptic-blending second-moment closure, Int. J. Heat Mass Transfer 48 (2005) 1583–1598.
[38] S.K. Choi, S.O. Kim, Computation of a turbulent natural convection in a rectangular cavity with the elliptic-blending second-moment closure, Int. Comm. Heat Mass Transfer 33 (2006) 1217–1224.
[39] J.K. Shin, J.S. An, Y.D. Choi, Elliptic relaxation second moment closure for turbulent heat flux, Proceedings of 4th International Symposium Turbulence and Shear Flow Phenomenon, Williamsburg, USA (2005) 271–277.
[40] S. Kenjeres, S.B. Gunarjo, K. Hanjalic, Contribution to elliptic relaxation modeling of turbulent natural and mixed convection, Int. J. Heat Fluid Flow 26 (2005) 569–586.
[41] S.V. Patankar, Numerical Heat Transfer and Fluid Flow, Hemisphere, New York, USA, 1988.
[42] J. Zhu, A low-diffusive and oscillation free convection scheme, Comm. Appl. Numer. Methods 7 (1991) 225–232.
[43] B. Van Leer, Towards the ultimate conservative difference scheme: Monotonicity and conservation combined in a second-order scheme, J. Comput. Phys. 14 (1974) 361–370.
[44] J. Smagorinsky, General Circulation experiments with the primitive equations: The basic experiment, Mon. Weather Rev. 91 (1963) 99–165.